Effects of gold on the properties of tin-antimony solder in flip-chip-pin-grid-array (FCGPA) packages

See Bee Kee[1], Luay B Hussain[1], Kesavan Nair[2], YL Khong [2,*], Dennis Chandran Prem Kumar[3]

[1] School of Materials & Mineral Resources Engineering, Univ Science Malaysia
[2] Asian Inst. for Medicine, Science & Technology, 2 Persian Cempaka, Amanjaya. 08000 Sg. Petani, Kedah, Malaysia
[3]Intel Technology (M) Sdn. Bhd, Malaysia

* Corresponding author: YL Khong [khong_yoon_loong@aimst.edu.my]

Abstract

The physical characteristics of tin-antimony solder used in FCPGA semiconductor packages change with the diffusion of gold from the gold plated layers in the solder pads or pin. This must be considered in the setting of parameters for subsequent re-flow processes and also possible impact on the quality and reliability of the solder joints. This paper describes physical and micro-structural properties of the 95Sn5Sb parent material alloyed with 1, 2, 2.5, 3, 3.5, 4 and 5 wt% of gold. In particular, the paper documents the decrease in the solidus and liquidus temperatures, increase in the Brinell hardness, and increase in both the electrical and thermal conductivity of 95Sn5Sb solder doped with gold.

Keywords

Soldering, Gold, Tin alloys, Antimony

1. INTRODUCTION

For applications in microelectronic packaging, dual solder systems are frequently used to allow for attachment of various parts at different stages of the packaging process. In the flip-chip-pin-grid-array (FCPGA) systems, the pins are soldered first to the organic substrate. The pin/solder joints must remain intact during the subsequent chip attach process, withstanding its reflow temperature.

Pin Grid Arrays (PGAs) are widely used in micro-processors (including Intel's Pentium IV's).

95Sn-5Sb has good electrical conductivity and mechanical strength [1]. The addition of antimony is known to have the desirable effect of retarding whisker growth and inhibiting allotropic transformation of tin [2] which ultimately weaken joint strengths. Together with its higher melting temperature, these properties make 95Sn-5Sb a good candidate for packages requiring dual solder systems for attachment of parts employing different processes. In the case of the FCPGA above, the 95Sn-5Sb solder (solidus temperature: 240^0C) for pin attachment and the 63Sn - 37Pb eutectic system (eutectic temperature: 183^0C) for chip attachment are appropriate selections.

Immersion deposition of gold on electro-less nickel layer over copper substrates is commonly used on electrical conductors in micro-electronic packages [3,4] . The thin layer of gold protects the underlying metal layers from oxidation and increases solder wetability and therefore adhesion. During the soldering process, the gold layer is fully consumed through diffusion into the tin base solder system [5]. The solder forms a joint with the nickel under-layer. However, with the high dissolution rate of gold in tin-containing solders, formation of $AuSn_4$ inter-metallic compound is often observed. Reflowing of solders containing high proportions of tin on gold plated layers shows significantly higher propensity for the formation of such intermetallic [6]. It is also found that with a thicker plated gold layer, more of the $AuSn_4$ inter-metallic is formed, which in turn affects the strength and reliability of the joints [7].

The tin-antimony solder system is used in electronic packages to join gold plated parts like the pins and pads mentioned earlier. It is thus important to understand the effects that addition of gold has, on the properties of the tin-antimony solder system and correlate the same to the subsequent processing involving the FCPGA packages.

In this work, the 95Sn5Sb solder doped with 1, 2, 2.5, 3, 3.5, 4 and 5 wt% of gold was characterized using its microstructure, melting behavior, electrical and thermal conductivity and hardness properties. The impact of such parameters on the processing of FCPGA packages is discussed.

2. MATERIALS AND EXPERIMENTAL PROCEDURE

The solder alloy materials of appropriate stoichiometry were purchased from Alpha Metals Inc.

A Perkin Elmer DSC7 was used for the thermal analysis using indium and tin for calibration purposes. The thermal profile employed comprises of a holding time of 1 minute at 190˚C followed by a ramp of 1ºC/min up to 250ºC.

Samples of 3x2x43mm were used for electrical conductivity measurements. The measurements were carried out using a Wheatstone Bridge circuit. The conductivity of the samples is expressed in terms of the International Annealed Copper Standard percentage (%IACS) [8].

Cylindrical specimens, nominally of 13.5 mm in radius and 31 mm in length were prepared for measuring the thermal conductivity using a heat conduction apparatus supplied by Armfield Limited. The heat flow throughout was maintained at 5 W.

For Brinell hardness testing, a tester by G. Melchrs & Co., Germany was used with an applied load of 62.5 kgf and a 5mm diameter ball.

For morphological studies an optical and scanning electron microscopy (SEM) were employed.

3. RESULTS AND DISCUSSION

3.1 DSC Studies:

The results of Differential Scanning Calorimetric (DSC) studies are given in Table 1. The same data is presented in Figures 1(a) and 1(b) as variations in solidus and liquidus temperatures as a function of Au additions to 95Sn5Sb solders. The solidus and liquidus temperatures of the 95Sn-5Sb with no gold content are 235.3 and 241.3^{o}C respectively which is in agreement with previous work [9]. With the addition of 1 wt% of gold, the solidus temperature falls rapidly to 214^{o}C. For subsequent increases in the gold content, the solidus temperature does not change appreciably. The liquidus temperature however decreases in an approximately linear fashion from 243 to 236^{o}C with the gradual incorporation of gold. These changes in the solidus and liquidus temperatures with gold content are consistent with the expected phase transitions of Au addition into Sn as shown in the phase diagram of Fig. 2 [10]. In the case of FCPGA packages, when gold plated

Table 1
The values obtained of the solidus and liquidus temperatures, electrical conductivity, thermal conductivity and Brinell hardness with wt% of gold in 95Sn-5Sb

Wt% of Au in 95Sn-5Sb	Solidus Temperature ± 0.5 (°C)	Liquidus Temperature ± 0.5 (°C)	Electrical Conductivity IACS %	Thermal Conductivity k (W/m-K)	Brinell Hardness Number
0	235.3	243.3	11.9	63.9	15
1	214.4	241.3	14	66.9	24.8
2	214.8	239.6	14.5	69.3	27.4
2.5	215.4	235.1	14.8	70.7	28.8
3	215.1	238.4	15.2	71.8	29.5
3.5	215.4	237.6	15.7	73.1	30.7
4	214.9	235.4	16	74.5	31.5
5	216	235.6	16.6	77.3	32.7

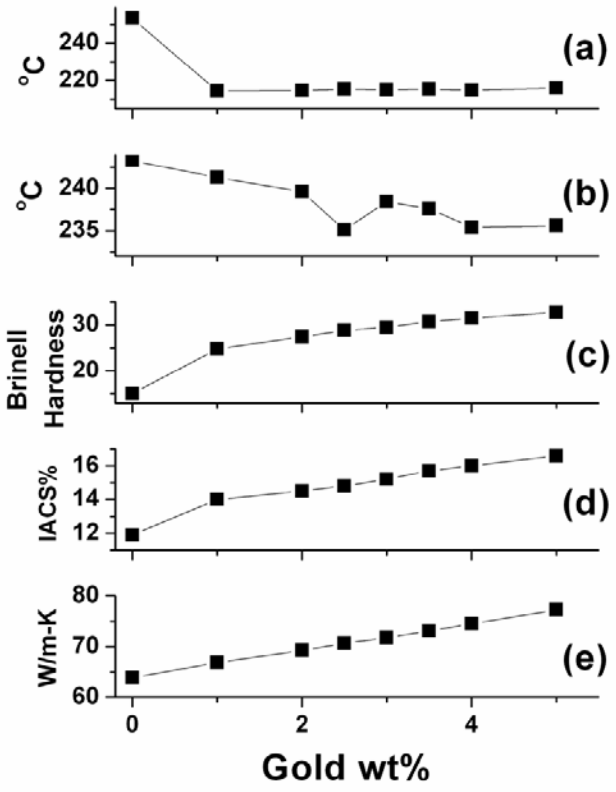

Fig.1 The variation of (a) solidus and (b) liquidus temperatures (c) Brinell hardness (d) electrical conductivity (e) thermal conductivity with wt% of gold content in 95Sn-5Sb solder material.

pins are attached to the substrate using the 95Sn-5Sb system, the pins tend to become loose from their original positions and in worst cases, drop off. In several instances, this occurred in the as received packages during the re-flow process for attaching the chip. This is consistent with the sharp fall in the solidus temperature observed with the incorporation of Au as mentioned, indicating that a tighter control over the re-flow temperatures is necessary when gold coated pins are being attached to the chips.

The above plots illustrate the dependency of the parameters investigated as a function of the level of gold doping. Hence, these plots show indirectly the dependency of these parameters with intermetallic formation.

3.2 Microstructure

The optical micrograph (at 100X) of the 95Sn5Sb and 1 and 5 wt% gold doped materials are shown in Figures 3(a) and 3(b) respectively. A SEM micrograph displaying the morphology of the inter-metallic more clearly is shown in Fig. 4. The elemental compositions of the various structures were confirmed by EDX.

The micrographs show the typical needle like $AuSn_4$ inter-metallic and aggregates of cuboids of SnSb in a dark etching matrix of primary solid solution of Au/Sb in Sn. The aggregates of the tin-antimony inter-metallic are better resolved in SEM micrographs; they are visible in optical micrographs as well.

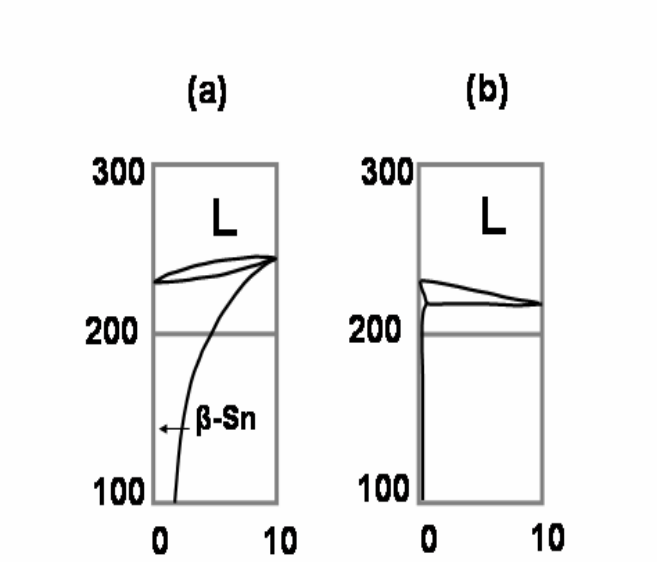

Fig. 2 The Sn – rich end of the phase diagram of (a) Sn/ Sb and (b) Au/95Sn5Sb for 0 – 10 wt% addition of Sb and Au respectively.

The optical micrographs show substantial increase in the density of the $AuSn_4$ inter-metallic with increasing gold doping. It is also apparent that this increase in the presence of the needle like $AuSn_4$ intermetallic has prevented segregation of the SnSb cuboids, as evidenced by the more uniform distribution of the aggregates (see Fig. 3(b)). At higher magnifications of the SEM micrographs, apart from a slight thickening of the $AuSn_4$ needles at 5 wt% doping, little change was observed in the morphology of the intermetallic on gold additions in the 1 to 4 wt% range.

Previous work has highlighted that the presence of $AuSn_4$ inter-metallic is of concern [11]. This was shown to weaken the solder joints significantly having adverse implications related to reliability issues. Apparently the beneficial effects of having a more even distribution of the SnSb intermetallic is nullified by the very presence of higher amounts of AuSn4 intermetallic. It is thus important to control the amount of gold from the parts to be joined to suppress the formation of this inter-metallic in the tin-antimony solder system.

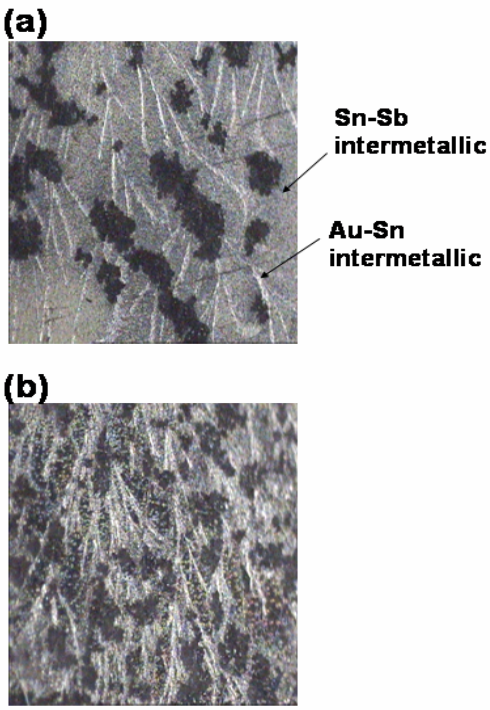

Fig. 3 The optical micrograph at 100x magnification of 95Sn5Sb solder material doped with a) 1wt% and b) 5wt% of gold. The Sn-Sb cuboids and needle shaped Au-Sn_4 inter-metallics appear as light aggregates and white strands respectively in a dark etching matrix of primary Sn solid solution.

3.3 Hardness

With increasing Au content from 0 to 5% in 95Sn-5Sb solder, the hardness as measured on the Brinell hardness scale increases from 15 to 32.7 (Table 1 and Fig. 1(c)). The rate of increase of hardness is apparently faster with the first 1% of Au incorporation. It has to be born in mind that the increase might not be linear in this range as shown – the slope of the line segment in this range is at best likely to be only a weighted average, since the solubility limit of Au is only about 0.3% in β-Sn at 200°C [12].

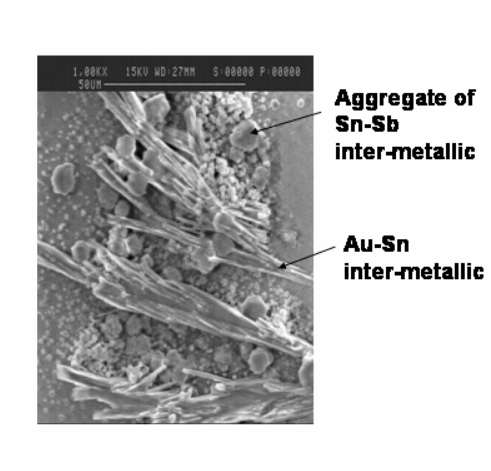

Fig. 4 SEM micrograph showing the needle shaped structure of $AuSn_4$ in 3% gold doped 95Sn-5Sb. Well resolved cuboids of SnSb are also clearly seen along with aggregates of the same.

This also implies that solid solution hardening might be the primary mechanism of hardening that is operative when gold additions remain low. However, beyond 0.3% of Au (involving the solubility limit of Au is about 0.3% in β-Sn at 200°C), hardening due to the introduction of the eutectic micro constituent will also play an increasingly predominant role. This explains why the later segment of the plot, beyond 1% Au, has a distinctly different slope.

Macro photographs of the fractured portion of the parent 95Sn-5Sb and Au doped materials shown in Fig. 5 reveals differences in the ductility. It is evident that the ductility is relatively low in case of samples containing Au, as shown by the absence of significant necking. The behaviour of the hardness characteristics discussed above broadly supports this conclusion.

It is thus expected that the increasing Au content would make the pin solder joints more susceptible to brittle fracture. Hence, pull or shear tests are recommended if joints are to be formed with parts involving gold plated surfaces using 95Sn-5Sb solders, especially if the gold plating thicknesses are not well determined.

3.4 Electrical and Thermal Conductivities

As shown in the Figures 1(d) and (e), as the doping of Au increases (and hence more intermetallic develops - refer to micrographs of Fig. 3), both the electrical and thermal conductivity increases. The joints therefore will have lower electrical and thermal resistance. The former perhaps is more critical in terms of performance since the resistance affects the speed of signal through a conductor. From the thermal consideration, the pins are not the main channels for heat dissipation. The values are also given in Table 1. In general, the incorporation of gold results in an increase in both thermal and electrical conductivities. The behavior of the plot is similar to that of hardness (Fig. 1(c)).

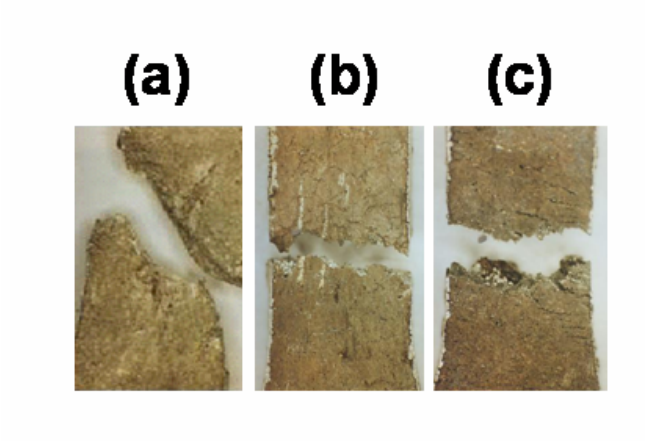

Fig. 5 Fracture patterns of a) 95Sn-5Sb parent material and parent material with b) 3 wt% and c) 5 wt% gold doping. Note the virtual absence of necking in the latter cases.

Arguments similar to those employed in that case are valid in this case also. However, it is well known that the conductivity of a solid solution, unlike hardness, decreases with solute content. This effect should have been detectable had the initial increments in gold additions were finer. Since the maximum solubility of gold in this system is only about 0.3%, an incremental addition of 1%Au might not be adequate to detect such finer details. Apparently the $AuSn_4$ intermetallic which is present in progressively higher amounts with increasing Au additions has a higher electrical conductivity than the Sn/Au solid solution. This increased conductivity is desirable from the electrical connectivity perspective especially for high speed electronic packaging.

The thermal conductivity increases in an apparently linear fashion from 63.9 to 77.3 W/m-K as the percentage of gold increases from 0 to 5. In the 0-1% range of Au doping, the trends of the thermal conductivity plot is different from those of hardness and electrical conductivity (Fig. 1(c) and 1(d)) in the sense that it does not show a significantly higher slope when compared to the later segments of the same plot. In general the degree of precision in case of thermal measurements is considerably less that that achievable in case of electrical measurements. In this case the difference in the rate of increase of thermal conductivity at lower and later ranges of Au addition might not be within

the detection accuracy of the equipment used. Nevertheless, these conductivities show a reasonably linear correlation for the corresponding gold doping levels with an R2 value of 0.97. This indicates that the Wiedemann-Franz law is by and large adhered to by this alloy system.

The results indicate a possible extra heat transfer to the extent of up to 20% from the chip through the substrate to the pins via the gold doped Sn-Sb solder. Any problems associated with this increase in heat transfer are not known. From the reliability perspective, increased heating of the pins hastens the degradation on the pin-socket connection. However, further work is required to investigate this aspect since pin-socket reliability is also dependent on other factors like moisture and contamination.

4. CONCLUSIONS

Parameters like hardness, electrical and thermal conductivity are sensitive to micro-structural changes involving the formation of the $SnAu_4$ inter-metallic. Beyond fractional percentages of Au additions, the changes in these parameters become by and large monotonic.

The ductility of the material decreases with gold additions as the presence of the eutectic micro constituent involving the $AuSn_4$ phase increases. The beneficial effect of a distinctly lower degree of segregation of the SnSb inter metallic as the network of $AuSn_4$ needles becomes well defined with increasing gold content, does not alter the situation significantly.

Together with the decreases in the solidus and liquidus temperatures, as predicted by the phase diagrams, this implies that the coating thickness and the reflow temperatures employed require tight control during the FCPGA packaging process using 95Sn-5Sb as pin solder.

Acknowledgements

Two of the authors (SBK and LBH) are grateful for a research grant provided by Intel Technology Malaysia to carry out this work.

References

[1] HH Manko, "*Solders and Soldering (3rd Edition)"*, New York, McGraw-Hill, pp. 133-136, 1992.

[2] A. Bornemann, "*Tin Disease in solder type alloys"*, ASTM Spec, Tech. Pub. 189, pp.129-148, 1956.

[3] FDB Houghton, "*ITRI project on electroless nickel/immersion gold joint cracking",* Circuit World vol 26 no 2 pp.10-16, 2000.

[4] Z Mei, P Johnson, M Kaufmann, A Eslambolchi, *"Effect of Ni/Immersion Au Plating Parameters on PBGA Solder Joint Attachment Reliability",* Proc. IEEE Electronics and Technology Conf., pp.125 1999.

[5] BF Dyson, "*Diffusion of gold and silver in tin single crystal",* J Appl. Phys., vol.37 no.6, pp.2375-2377, 1966.

[6] [CE Ho, SY Tai and CR Kao, "*Reaction of Solder with Ni/Au Metallization for Electronic Packages During Re-flow Soldering",* IEEE Trans on Adv. Packaging, Vol. 24, no.4, pp. 493-498, November 2001.

[7] JR Ganasan, "*Soldering on Gold Plated Substrates-Solder Joint Reliability and Integrity of Surface Components",* IEEE Intl. Elec. Manuf. Tech. Symp., pp.372- 376, 1995.

[8] International Electrotechnical Commission Publication No. 28, 1913.

[9] S Akram, "*Lead-Free Eleectronics : Searching for a Lead free Replacement",* Future Fab Intl, vol. 9, 2000.

[10] J. H. Vincent, B.P. Richards "*Alternative Solders for Electronics Assemblies"* Circuit World, vol.19, No.3, pp.33, 1993

[11] Z Mei, M Kaufmann, A. Eslambolchi and P. Johnson, "*Brittle Interfacial fracture of PBGA packages soldered on electroless Nickel/Immersion Gold"* in Proc. 48th IEEE Electron. Comp. Tech. Conf., pp. 952-961, 1998

[12] E. Jenkel and L. Roth Z Metallkd 30(1938) 135-144